

Latent Fingerprint Matching: Utility of Level 3 Features

Qijun Zhao, Jianjiang Feng, and Anil K. Jain, *Fellow, IEEE*

Abstract

Automatic fingerprint identification systems (AFIS) have for a long time used only minutiae for fingerprint matching. But minutiae are only a small subset of fingerprint detail routinely used by latent examiners for fingerprint matching. This has generated a lot of interest in extended feature set (EFS) with the aim of narrowing down the gap between the performance of AFIS and latent examiners. Level 3 features constitute the most significant subset of extended features. Studies on level 3 features have reported significant improvement in the fingerprint recognition accuracy. However, these studies were based either on live-scan fingerprints or full (rolled or slap) fingerprints. As a result, the conclusions of these studies cannot be extended to latent fingerprints, which are characterized by small size, poor image quality, and severe distortion compared to full fingerprints. In this paper, we study the utility of level 3 features, including pores, dots, incipient ridges, and ridge edge protrusions, for latent matching. Automatic algorithms for extracting and matching these features are proposed. While most existing level 3 feature matching algorithms only consider the locations of features, the proposed method utilizes the topological relationship between level 3 and level 2 features, and is thus robust to nonlinear distortion and has high discriminative capability. Given the proposed algorithms and operational latent fingerprint databases, we identify the challenges in using level 3 features, and show the potential of level 3 features in improving latent matching accuracy. Further, by using simulated partial fingerprints, we highlight that level 3 features can indeed improve latent matching accuracy when i) level 3 features can be reliably extracted in both latent and full fingerprints and ii) latent fingerprints have only a small number of minutiae or the minutiae match scores are low. With the increasing adoption of 1000ppi fingerprint scanners in law enforcement agencies, it is becoming feasible and desirable to incorporate level 3 features into AFIS. We believe that the proposed algorithms and analysis will be useful in the design and development of next generation AFIS.

Index Terms

Latent fingerprint matching, extended features, level 3 features, forensics



1 INTRODUCTION

Fingerprint recognition has been accepted as a reliable person identification technique for almost 100 years. Fingerprints are now routinely used worldwide to identify suspects and victims in law enforcement and forensics [1]. The demand for Automatic Fingerprint Identification Systems (AFIS) became compelling in the early 1960s, because of the rapid expansion of fingerprint recognition in law enforcement and the ever-increasing size of fingerprint databases (e.g. the FBI fingerprint database now has more than 800 million fingerprint images) [2]. Many automatic algorithms have been proposed for extracting and matching fingerprint features, and a large number of AFIS are successfully deployed not only for forensic applications, but also for many emerging civilian and commercial applications [1][2].

Three types of fingerprint images are commonly used in law enforcement applications: ink, live-scan, and latent (see Fig. 1). The inking method is the earliest method for capturing and recording fingerprints. To capture the ink fingerprint images of a subject, the finger is coated with ink and pressed or rolled against a paper card. The print left on the card is then scanned to obtain a digital fingerprint image. Live-scan fingerprint images are obtained by using optical, capacitive, or other types of sensors to directly image the finger. Latent fingerprint images are inadvertently left by persons on surfaces of objects and are lifted or photographed by using various techniques, e.g. chemical processing [1]. Compared to ink and live-scan fingerprint images, latent fingerprint images are characterized by small area, poor quality, and large non-linear distortion [17].

Fingerprint features can be generally divided into three levels [2], as shown in Fig. 2. Level 1 features are defined by fingerprint ridge flow and general morphological information, e.g. ridge orientation field, ridge pattern types, and singular points. These features are not unique to each finger and are primarily used for fingerprint type classification (e.g. whorl, left loop, right loop, and arch) and indexing. Level 2 features refer to individual fingerprint ridges and fingerprint ridge events, such as minutiae. There are two prominent types of minutiae, i.e. ridge endings and ridge bifurcations. Level 2 features are quite discriminative and stable. Level 3 features are defined as fingerprint ridge dimensional features. Pores,

-
- *Qijun Zhao and Anil K. Jain are with the Department of Computer Science and Engineering, Michigan State University, East Lansing, MI, 48824, United States.
E-mail: {qjzhao, jain}@cse.msu.edu*
 - *Jianjiang Feng is with the Department of Automation, Tsinghua University, Beijing 100084, China.
Email: jfeng@tsinghua.edu.cn*

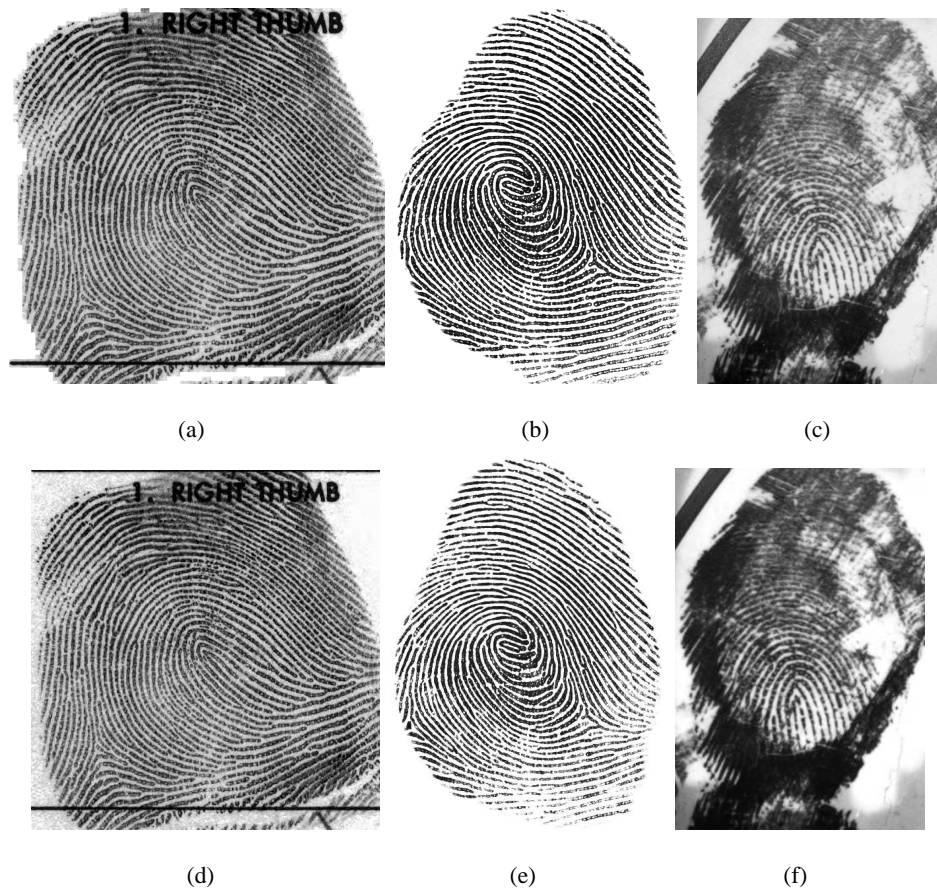


Fig. 1. Three types of fingerprint images: (a, d) Ink, (b, e) live-scan, and (c, f) latent fingerprints. (a-c) are 1000 ppi, and (d-f) are the corresponding 500 ppi images.

dots, incipient ridges, and ridge edge shapes are typical level 3 features¹. These features, if present and reliable (assuming that the input image is of good quality), are also quite distinctive [3][4]. While level 1 and level 2 features can be extracted from the standard 500 ppi (pixels per inch) fingerprint images, extraction of level 3 features usually require higher resolution (at least 1000 ppi) images [2][5][18] (see Fig. 1). As a result, the current AFIS technology, which relies on 500 ppi images, mainly utilizes level 1 and level 2 features [2][7]. Latent fingerprint experts, on the contrary, often rely on additional level 3 information due to the limited level 1 and level 2 (i.e. minutiae) information available in many latents [3][25] (see Fig. 3). It has been suggested that one way to improve the AFIS performance is to utilize level 3 features [6]. In response to this, the Committee to Define an Extended Fingerprint Feature

1. Although it is debatable at which level dots and incipient ridges belong, we classify them into level 3 features.

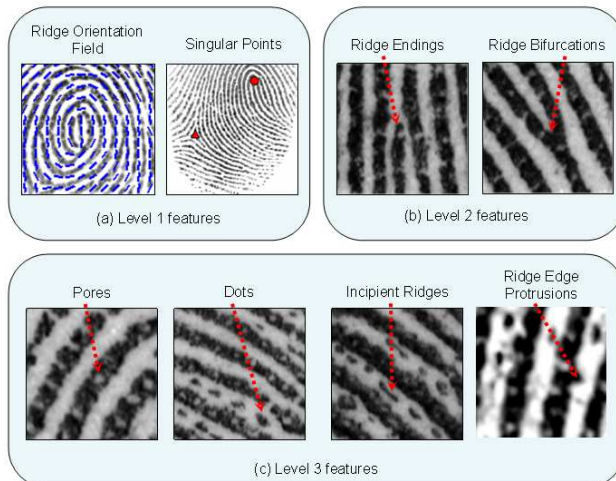


Fig. 2. Fingerprint features: (a) Level 1 (ridge orientation field and singular points), (b) level 2 (minutiae, i.e. ridge endings and ridge bifurcations), (c) and level 3 (pores, dots, incipient ridges, and ridge edge protrusions).

Set (CDEFFS) was chartered to define the next ANSI/NIST-ITL standard [5] so that extended features, including the level 3 features, can be utilized in the next generation AFIS. Meanwhile, the availability of high resolution (1000 ppi) fingerprint image scanners also makes it feasible to incorporate level 3 features into AFIS.

1.1 Related Work

Among the various level 3 features, pores have received the most attention. Stosz and Alyea [8] proposed the first pore-based fingerprint matcher. Kryszczuk et al. [9] studied the effectiveness of pores in matching small fragmentary fingerprints to full fingerprint templates on a small 2000ppi fingerprint image database. Jain et al. [10] utilized fingerprint features at each of the three levels, including minutiae and pores. The International Biometric Group [14] studied the effectiveness of pores by using the algorithm in [10] to extract pores and using the minutiae matcher in the NIST Biometric Image Software [24] to match pores. Zhao et al. [11][12] proposed pore extraction and matching methods and applied them to partial and full high resolution fingerprint matching. All these studies reported that fusion of pores with minutiae does improve the fingerprint matching accuracy. However, these studies considered only live-scan fingerprint images, and their matching experiments did not use a state-of-the-art fingerprint matcher as a baseline.

A very limited number of studies on other types of level 3 features have also been reported. Chen

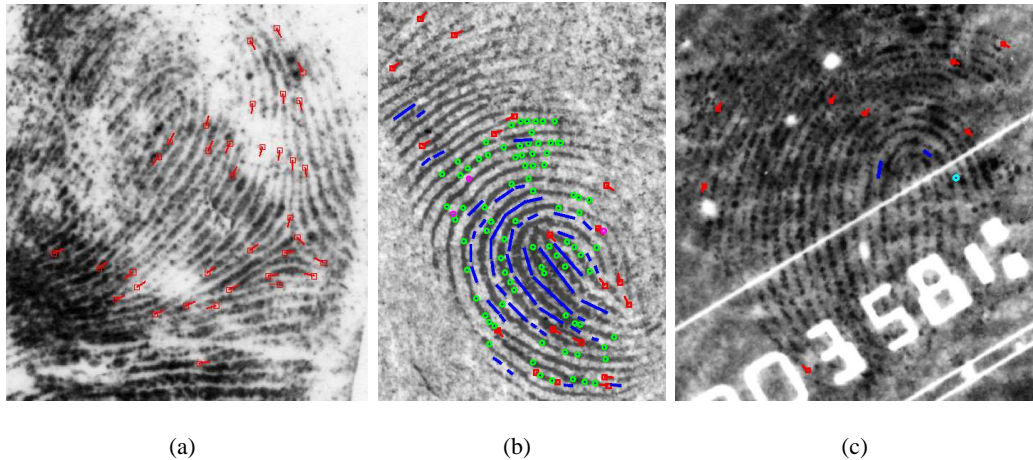


Fig. 3. Some example latent fingerprints from the ELFT-EFS-PC database. Minutiae (marked by red rectangles), pores (green circles), dots (cyan circles), incipient ridges (blue lines), and ridge edge protrusions (magenta circles) in latents were manually marked by latent experts. Some latents may have a small number of minutiae together with some extended features (c). In the ELFT-EFS-PC database (255 latents), there are, on average, about 18 minutiae in a latent, compared to 133 minutiae in a rolled ink fingerprint in the background database (4180 full fingerprints). Some latents in this database have only 4 minutiae.

and Jain [13] obtained promising results in matching dots and incipient ridges extracted from partial fingerprints cropped from NIST SD30. The International Biometric Group [14] also investigated the sampled points on ridge contours and ridge edgeoscopic features (i.e. high curvature points on ridge edges) for high resolution (2000ppi) fingerprints. These features were treated as minutiae and matched using the minutiae matcher in the NIST Biometric Image Software [24]. Neither of these two studies designed special algorithms for matching level 3 features, but instead completely relied on existing minutiae matchers. Zhou et al. [15] studied the creases in fingerprints and experimentally showed their effectiveness in improving the recognition accuracy of fingerprints of elderly subjects (aged between 46 and 95, with an average age of 67). Although a significant improvement in the fingerprint recognition accuracy was observed in all these studies, their conclusions cannot be simply applied to latent fingerprint matching due to the huge difference in the characteristics of latent fingerprints and full fingerprints.

The National Institute of Standards and Technology (NIST) has conducted an extensive evaluation of latent fingerprint technologies (ELFT) [16]. Extended feature sets (EFS) were manually marked in the

latent fingerprints, and their contribution to latent search was assessed by using a number of commercial AFIS provided by the vendors who participated in the program. The NIST evaluation showed that EFS did improve the latent search accuracy. However, because the ELFT-EFS test did not evaluate each extended feature separately, the contribution of individual level 3 features could not be determined from this evaluation. Jain and Feng [17] examined the extended features at level 1 and level 2, i.e. singularity, ridge quality, ridge orientation field, ridge wavelength, and ridge skeleton, for latent matching using 500 ppi latent images in NIST SD27. They also studied the statistics of some of the level 3 features, including pores, dots, and incipient ridges. By manually marking and aligning these features in 500 ppi latent and exemplar fingerprint images in NIST SD27, they observed a very small number of mated level 3 features. Based on this, they concluded that these level 3 features do not improve the latent matching accuracy, at least on the NIST SD27 database. In summary, the small number of studies on latent fingerprint matching do not provide specific guidelines on the utility of level 3 features in improving latent matching accuracy.

1.2 Contributions of This Paper

The goals of this study are i) design level 3 feature extraction and matching algorithms, ii) determine the utility of level 3 features in latent matching, iii) explore how to incorporate level 3 feature matchers into existing AFIS, and iv) make recommendations regarding the effectiveness of level 3 features. To achieve these goals, we propose a novel algorithm for matching level 3 features in small area latent fingerprints, and systematically determine the relative contribution of level 3 features in improving the latent matching accuracy. In particular, the utility of pores, dots, incipient ridges, and ridge edge protrusions is studied for latent search. With the proposed algorithms and available latent databases, i.e. ELFT-EFS-PC (ELFT-EFS Public Challenge Dataset [16]) and WVU (West Virginia University), we identify the challenges in using level 3 features, and show the potential of level 3 features in improving latent matching accuracy. Further, we highlight the cases where level 3 features can significantly improve latent matching accuracy by using simulated partial fingerprints. The main contributions of this paper are

- Design of a topological level 3 feature matching algorithm for latent to full fingerprint matching. Instead of considering only the locations of level 3 features, the proposed method enforces the topological relationship between level 3 features, minutiae, and ridges. It is thus robust to image distortion which is frequently observed in latents;
- Based on an analysis of latent fingerprint databases and results of experiments on both latent and simulated partial fingerprint images, we show that level 3 features in available latent databases are of limited use because the poor quality of exemplar fingerprints in these databases seriously degrades

the reproducibility of level 3 features;

- We empirically determine the situations where level 3 features show promise in improving latent matching accuracy.

The rest of the paper is organized as follows. Sections 2 and 3 introduce the proposed extraction and matching algorithms for level 3 features, respectively. Section 4 presents and analyzes the experimental results. Section 5 concludes the paper.

2 LEVEL 3 FEATURE EXTRACTION

Level 3 fingerprint features considered here include pores, dots, incipient ridges, and ridge edge protrusions. Pores appear as bright blobs on ridges and the other three features appear between ridges (see Fig. 2(c)). We first discuss pore extraction, followed by extraction algorithm for the other three features.

2.1 Pores

Pores, also known as sweat pores, are located on finger ridges. They are formed in the sixth month of gestation due to the sweat-gland ducts reaching the surface of the epidermis. Once the pores are formed, they are fixed on the ridges; typically, there are between 9 and 18 pores along a centimeter of a ridge [2]. A pore can be visualized as open on one print, but as closed on another print of the same finger depending on the finger pressure and whether it is exuding perspiration. As shown in Fig. 2(c), a closed pore appears as an isolated dot on the ridge, while an open pore is connected to one or both of the two valleys surrounding it. As a result, the shape and size of pores can vary from one impression to another, and therefore only the pore position is used in matching.

The basic idea of the proposed pore extraction method is to model the spatial appearance of pores in fingerprint images and detect them via filtering the images with suitable matched filters. In [11], it was shown that along the ridge tangential orientation, the intensity profile across the pore has a Gaussian shape irrespective of whether it is open or closed (see Figs. 4(a) and 4(b)). Based on this observation, an anisotropic pore model was established and an adaptive pore extraction algorithm was proposed [11]. One drawback of the method is that it sets the scale parameter in the pore model as a constant multiple of local ridge period. However, such a constant ratio parameter is difficult to specify for all fingerprints, especially when large distortion exists across the fingerprint images, such as with latent prints. As an improvement to the method in [11], we propose a new pore matched filter based on the automatic scale selection technique [20]. Let X and Y be the horizontal (column) and vertical (row) axes of the global image coordinate system (x and y are the corresponding coordinates), and V and U denote the local

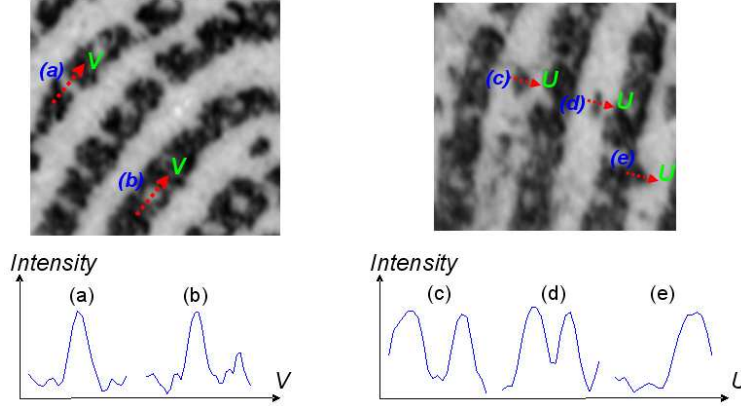


Fig. 4. Properties of level 3 features. (a) and (b): Intensity profile across a pore along the ridge tangential orientation has a Gaussian shape. (c), (d), and (e): Intensity profile across a dot, an incipient ridge, or a ridge edge protrusion along the ridge normal orientation has the shape of a full or half negative Gaussian.

ridge tangential and normal orientation, respectively. Let θ be the local ridge (tangential) orientation with respect to the X axis. The proposed pore matched filter is defined as

$$P_{POR}^{\gamma}(v, u; t_V, t_U, \theta) = -t_V^{3/4} g_{VV}(v; t_V) g(u; t_U), \quad (1)$$

where

- $(v, u) = (x \cos \theta - y \sin \theta, x \sin \theta + y \cos \theta)$,
- $g(u; t_U) = 1/(\sqrt{2\pi t_U}) e^{-u^2/(2t_U)}$ is Gaussian along the ridge normal orientation and constant along the ridge tangential orientation,
- $g_{VV}(v; t_V) = (v^2 + t_V)/(\sqrt{2\pi t_V^5}) e^{-v^2/(2t_V)}$ is Laplacian along the ridge tangential orientation and constant along the ridge normal orientation,
- and t_V and t_U are, respectively, the variances along the ridge tangential orientation and the ridge normal orientation.

Note that unlike [11], we describe the intensity appearance of a pore along the ridge tangential orientation by using a Laplacian kernel because it is more robust to noise. The Gaussian kernel along the other orientation is used merely for smoothing the noise along the ridge normal orientation.

In order to apply the above pore matched filters, we first divide the fingerprint image into blocks and estimate the local ridge orientation θ . We then instantiate a pore matched filter for each block that has dominant ridge orientation (called a well-defined block) according to eq. 1. The parameter t_U in the pore

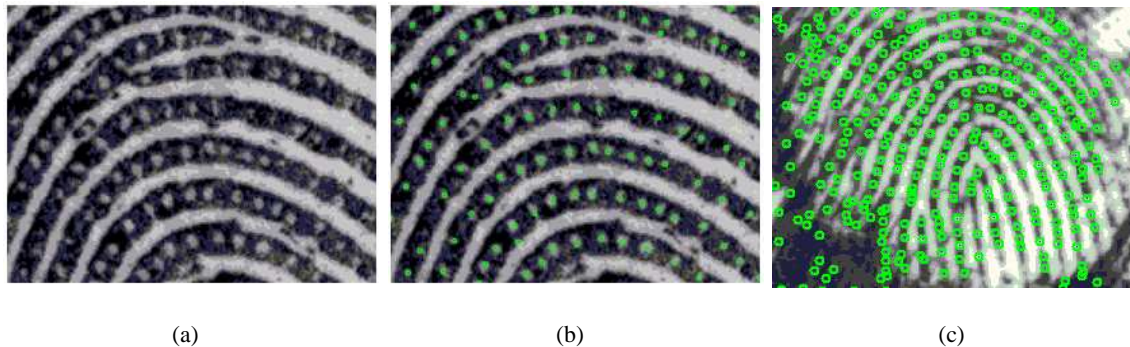


Fig. 5. Example pore extraction results. (a) Part of a rolled ink fingerprint image in NIST SD30. (b) Pores detected in (a). (c) Pores detected in the latent fingerprint image in Fig. 1(c).

matched filter is set to a constant because it is used merely for noise smoothing. As for the parameter t_V , a multiscale setting is adopted so that pores of varying sizes can be detected. More specifically, a set of pore matched filters are constructed for each well-defined block and convolved with the block. The maximum response among the sets of pore matched filters is binarized, resulting in the pore map; candidate pore pixels have value 1 and the non-pore pixels have value 0.

The pore map contains some falsely detected pores. To remove them, the following post-processing steps are conducted: (i) candidate pores which are not on ridges are removed; (ii) connected components on the pore map whose area is either too small or too large are discarded; (iii) connected components on the pore map are removed if the intensity of their pixels is too low. After these post-processing operations, many spurious pores are excluded, and each connected component in the post-processed pore map corresponds to a pore. The centroids of these detected pores are recorded. Fig. 5(a) shows a portion of a rolled ink fingerprint image, and Fig. 5(b) shows the pores detected in it by the proposed method. The pore extraction results of the latent fingerprint image in Fig. 1(c) are shown in Fig. 5(c). Due to the poor quality of latent fingerprint images, more false pores are detected in the latent than in the rolled image. Yet, most of the true pores are correctly extracted in latents. Therefore, the automatic pore extraction algorithm proposed here may provide useful information to latent examiners and cut down their workload of manually marking pores.

2.2 Dots, Incipient Ridges, and Ridge Edge Protrusions (DIP)

While typical ridges stretch over a large area of a fingerprint and their width varies from $100\mu m$ to $300\mu m$ [2], there are occasionally some ridges which are quite short or substantially thin (see Fig. 2(c)). These

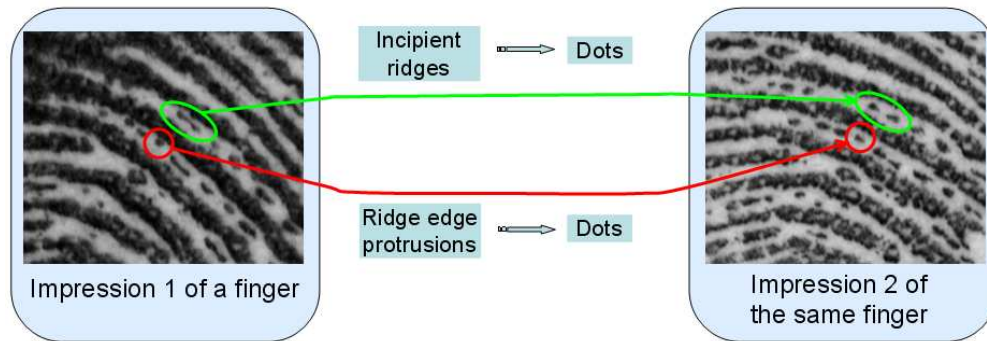


Fig. 6. Dots, incipient ridges, and ridge edge protrusions are easily confused with each other in different impressions of the same finger. We thus unify them into a single feature type.

are actually dots and incipient ridges, two additional types of level 3 features in fingerprints [5]. Unlike pores, which are present in almost every finger, dots and incipient ridges can be found in fingerprints of only about 45% of the population and 13.5% of the fingers [13]. They reside in fingerprint valleys and, if observed in small areas, have been claimed to be distinctive for differentiating fingerprints.

Along a ridge, variations in ridge width can be observed. This gives rise to ridge edge features, including protrusions, indentations, and discontinuities (see Fig. 2(c)), among which protrusions are the most notable ridge edge feature [5]. A ridge edge protrusion refers to an abrupt increase in ridge width that is not long enough to be called a bifurcation. Although ridge edge protrusions, dots, and incipient ridges are defined as different features, their appearance in fingerprint images can be greatly affected by finger pressure and imaging conditions [13], and consequently, they can be confused with each other in different impressions of the same finger. As shown in Fig. 6, a dot in one impression can appear as a ridge edge protrusion in the other impression, and an incipient ridge can appear as a series of separated dots. Therefore, we do not distinguish among these three types of level 3 features for extraction and matching, but collectively label them as a single feature type (denoted as DIP).

In order to extract the DIP features, a procedure similar to that for pore extraction is applied, but with matched filters designed for DIP. Fig. 4 shows that the intensity profiles along the ridge normal orientation are shaped as a full or half negative Gaussian. Therefore, we define the following matched filters for the DIP features,

$$P_{DIP}^{\gamma}(v, u; t_V, t_U, \theta^{\perp}) = t_U^{3/4} g(v; t_V) g_{UU}(u; t_U), \quad (2)$$

where θ^{\perp} is the local ridge normal orientation at the DIP feature (perpendicular to θ). The DIP matched

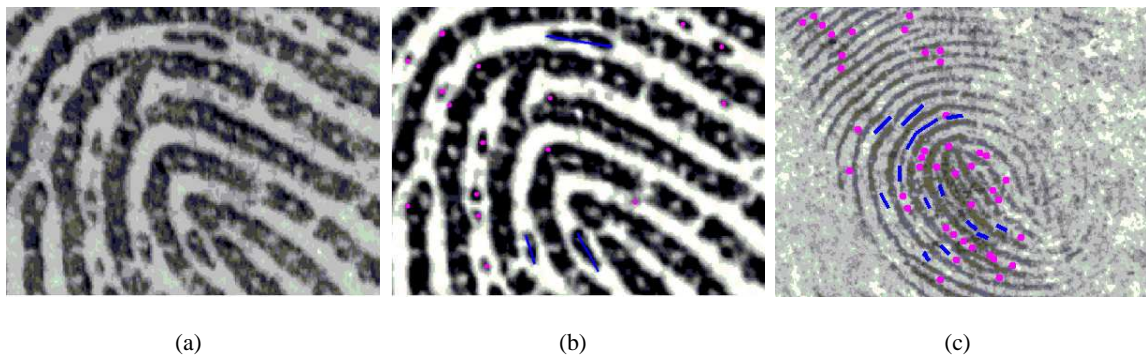


Fig. 7. Example DIP extraction results. (a) Part of a rolled ink fingerprint image in NIST SD30. (b) DIP features detected in (a). (c) DIP features detected in the latent fingerprint image in Fig. 3(b).

filters are applied for each block that has dominant ridge orientation with t_V set to a constant, and t_U to a multiscale setting. The resulting DIP map then goes through the following post-processing steps. First, the candidate DIP pixels which are not in the valleys are removed, because the DIP features should reside in valleys only. Second, the connected components in the DIP map of either too small or too large area are discarded. Third, those components in the DIP map whose intensity is too high are removed. After these post-processing operations, many spurious DIP are excluded. The remaining connected components in the DIP map are then thinned to single-pixel curves. If a curve bends too much, i.e. the maximum distance from its pixels to the chord (straight line connecting its two ends) is too large, it is divided into two curves at the pixel which is farthest from the chord. Finally, the centroids of these curves are recorded to represent the extracted DIP features in the fingerprint. The DIP extraction results of the proposed method for an example rolled ink fingerprint fragment are shown in Fig. 7(a) and Fig. 7(b) (note that if the length of a detected DIP is larger than the local ridge period, it is displayed as an incipient ridge. See the blue lines in Fig. 7(b)). The DIP extraction results in the latent fingerprint image in Fig. 3(b) are shown in Fig. 7(c). Despite the poor quality of the latent, most of the true DIP features have been correctly extracted by the proposed method, but there are many false detections (most of which are due to ridge edge features).

3 LEVEL 3 FEATURE MATCHING

3.1 Algorithm Overview

Given a latent fingerprint, it is first matched with the exemplars in the background database by using a minutiae matcher (VeriFinger [19] was used in our experiments). The rank 1 minutiae match score is

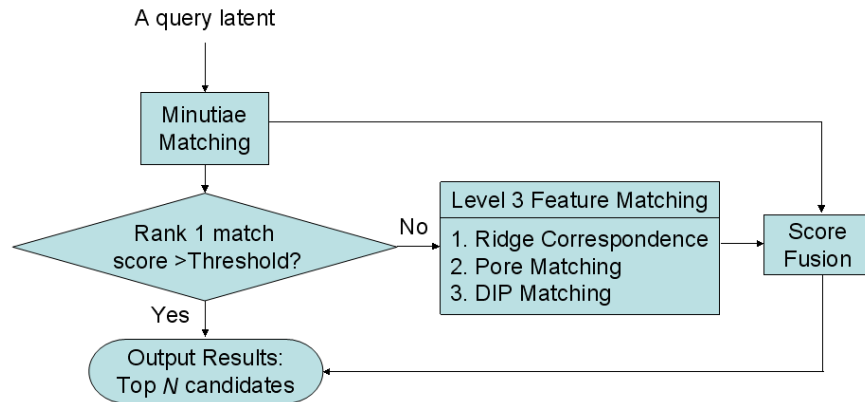


Fig. 8. An overview of the proposed latent fingerprint matching algorithm which utilizes level 3 features.

then examined to determine if it is necessary to invoke the level 3 feature matching module. Specifically, if the rank 1 minutiae match score is already above a prespecified threshold, the matcher will directly output the identification results (e.g. the list of top N candidates); otherwise, the level 3 features will be further compared, and the final identification results will be based on the fusion between the matching results of minutiae and level 3 features. Fig. 8 illustrates this algorithm.

We first match the minutiae because i) minutiae have already been shown to be stable and discriminative, and ii) minutiae form the basis of all the available AFIS. In the rest of this section, we will describe the three modules of the proposed level 3 feature matching method, i.e. ridge correspondence establishment, pore matching, and DIP matching.

3.2 Ridge Correspondence Establishment

The level 3 feature matching method proposed here differs from existing methods in that it matches level 3 features along the ridges and incorporates the topological relationship between level 3 features, minutiae, and ridges. Given a query latent F_q and an exemplar full fingerprint F_t , the proposed matcher first establishes the ridge correspondences between the two fingerprints. To facilitate the ridge matching process, the ridges in each fingerprint are traced and sampled at a constant interval (in our experiments, the interval is set to 10 pixels, which is the allowed tolerance of location displacement between two matched level 3 features). During the ridge tracing and sampling, the associated minutiae (if any) are recorded for each of the ridges, and the neighboring ridges and the neighboring sampling points on the left-hand and right-hand sides at each sampling point of the ridge are also recorded.

Algorithm 1 Ridge Correspondence Establishment

Input: MM : Mated minutiae pairs between F_q and F_t ; R_q, R_t : Ridges in F_q and F_t **Output:** s_r : Similarity between ridges in F_q and F_t ; MR : Mated ridge pairs between F_q and F_t , and corresponding sampling points on them

```

1:  $s_r \leftarrow 0, MR \leftarrow \text{NULL}$ 
2: for each pair of mated minutiae,  $\{M_1, M_2\}$ , in  $MM$  do
3:   for each pair of ridges,  $\{R_1, R_2\}$ , associated with  $M_1$  and  $M_2$  do
4:     Generate candidate aligned ridge pairs  $CR = \{RSP_1, 0, RSP_2, 0\}$  from  $\{R_1, R_2\}$ 
5:      $MRSP \leftarrow \text{IntraRidgeMatch}(CR)$ 
6:     if  $|MRSP| > 4$  then
7:        $(mr, s) \leftarrow \text{InterRidgePropagation}(R_q, R_t, MRSP)$ 
8:       if  $s_r < s$  then
9:          $s_r \leftarrow s, MR \leftarrow mr$ 
10:      end if
11:    end if
12:  end for
13: end for

```

Algorithm 1 describes the ridge correspondence establishment. Suppose a set of mated minutiae are found between F_q and F_t by the minutiae matcher. Fig. 9 shows an example latent and its mated rolled fingerprint in ELFT-EFS-PC. There are three pairs of mated minutiae in them. From each pair of mated minutiae, several pairs of candidate aligned ridges can be obtained from the ridges associated with the two minutiae in the pair. A candidate aligned ridge pair is defined as $CR = \{RSP_1, PR_1; RSP_2, PR_2\}$, where RSP_1 and RSP_2 are the two candidate ridges (or ridge segments) represented by their sampling points and the first sampling points on them are assumed to be matched (here, the sampling points corresponding to the mated minutiae) and PR_1 and PR_2 are the parent ridges from which this candidate aligned ridge pair is generated. For the candidate aligned ridge pairs generated from mated minutiae, the parent ridges are set to 0, which means they have no parent ridges. The parent ridges will be used in Inter-Ridge propagation to ensure that only the sampling points neighboring to the parent ridges are matched during the propagation. For example, for the mated minutiae pair $\{F_q.M_1, F_t.M_1\}$ in Fig. 9(a), each of the three ridges associated with $F_q.M_1$ is paired with the corresponding ridge associated with

$F_t.M_1$, resulting in three pairs of candidate aligned ridges. Note that if a ridge ending is mated with a ridge bifurcation, we will have two pairs of aligned ridges, while if two ridge endings are mated, we will get only one pair of aligned ridges.

From each of these aligned ridge pairs, the two ridges in the pair are first compared by the Intra-Ridge matching procedure. If the two ridges can be matched (i.e. more than four sampling points are matched between them), the Inter-Ridge propagation procedure is invoked to match the remaining ridges in the two fingerprints based on the mated sampling points on the two ridges. After all the aligned ridge pairs have been considered, the ridge correspondences obtained from the one which gives the highest similarity between the ridges in the two fingerprints are taken as the final result. Next, we introduce the two main procedures, Intra-Ridge matching and Inter-Ridge propagation, which are involved in ridge correspondence establishment.

3.2.1 Intra-Ridge Matching

Given a candidate aligned ridge pair $CR = \{RSP_1, PR_1, RSP_2, PR_2\}$, Intra-Ridge matching is used to find the corresponding sampling points on the two aligned ridges (or ridge segments). This is essentially a string matching problem given that the first sampling points in RSP_1 and RSP_2 are matched. We employ the dynamic programming technique [21] to find the longest sequence of mated sampling points on the two ridges, $MRSP = \{RSP_1^m, RSP_2^m\}$, such that (i) the indices of mated sampling points monotonously increase in both RSP_1^m and RSP_2^m , (ii) changes between indices of adjacent mated sampling points are less than 3 (i.e. no more than 3 sampling points can be skipped during matching), and (iii) if $PR_i \neq 0$, all the mated sampling points in RSP_i^m should have PR_i as their neighboring ridges ($i = 1, 2$). In our implementation, two mated sampling points should satisfy i) the absolute difference between the distances from them to the first sampling points is below a given threshold (i.e. 10 pixels), and ii) the absolute difference between the ridge curvatures at them is also below a given threshold (i.e. 15 degrees). We measure the distance between two sampling points on a ridge by using the absolute difference between their indices, which is similar to geodesic distance. The ridge curvature at a sampling point is measured by the change in local ridge orientation at the point with respect to the ridge orientation at the first sampling point.

Given the mated points between two ridges, the similarity between the ridges is computed as follows. Because short ridges are mostly unreliable, if there are fewer than 4 mated points between two ridges, we discard them. Otherwise, we further examine the neighboring ridge structures of the mated sampling points. Let $n_{msp} = |MRSP|$ be the number of mated sampling points found on RSP_1 and RSP_2 .

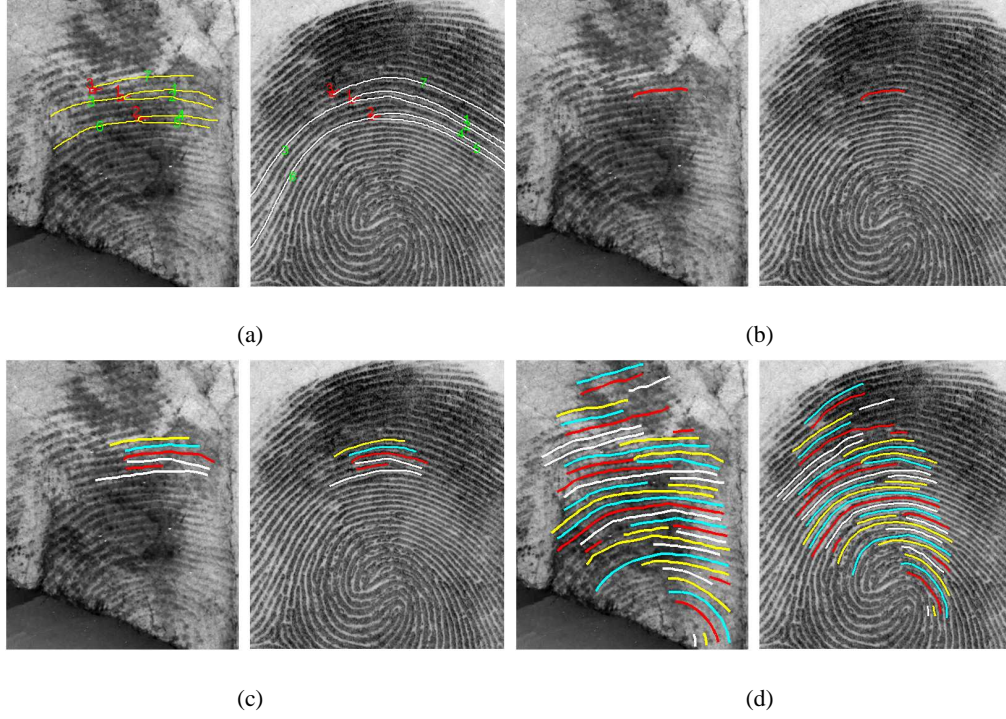


Fig. 9. Ridge correspondence establishment results for the latent L177B and its mated exemplar in ELFT-EFS-PC. (a) Three pairs of mated minutiae are found between the latent and its exemplar. (b) The ridges $F_q.R_1$ and $F_t.R_1$ associated with the mated minutiae pair $\{F_q.M_1, F_t.M_1\}$ are matched by Intra-Ridge matching. (c) The mated ridges found at an intermediate step as the procedure Inter-Ridge propagation proceeds from the mated ridges in (b). (d) The final mated ridges between the two fingerprints obtained by the proposed method. Corresponding ridges are marked by the same color.

For all the mated sampling points in $RSP_i^m (i = 1, 2)$, we examine on left-hand and right-hand sides, respectively, if the neighboring ridges of each two adjacent sampling points are different or not, resulting in two feature vectors, $NR_i^l \in \{0, 1\}^{n_{msp}-1}$ and $NR_i^r \in \{0, 1\}^{n_{msp}-1}$, in which ‘0’ means same ridge and ‘1’ means different ridges. NR_1^l and NR_1^r are then compared with NR_2^l and NR_2^r , respectively, and the number of the same entries between them is counted, denoted as n_{NR}^l and n_{NR}^r for the left-hand and right-hand sides, respectively. The similarity between the neighboring ridge structures of the mated sampling points on the two ridges is then calculated by

$$s_N = 0.5 \times \frac{n_{NR}^l}{n_{msp} - 1} + 0.5 \times \frac{n_{NR}^r}{n_{msp} - 1}. \quad (3)$$

If the mated sampling points on the two ridges have very low similarity between their neighboring ridge structures, they are also discarded. Fig. 9(b) shows the Intra-Ridge matching results for the ridges $F_q.R_1$ and $F_t.R_1$ associated with the mated minutiae $F_q.M_1$ and $F_t.M_1$ in Fig. 9(a).

3.2.2 Inter-Ridge Propagation

Given a set of mated sampling points on the two ridges found by the Intra-Ridge matching procedure, the Inter-Ridge propagation procedure, as sketched in Algorithm 2, matches all the remaining ridges. A queue (denoted as Q) is constructed to store the candidate aligned ridge pairs. The queue is initialized by generating candidate aligned ridge pairs from each pair of mated sampling points. The candidate aligned ridge pairs are the neighboring ridges on the corresponding sides of the mated sampling points.

Algorithm 2 Inter-Ridge Propagation

Input: $MRSP$: Mated sampling points on two ridges in F_q and F_t ; R_q, R_t : Ridges in F_q and F_t

Output: s_r : Similarity between ridges in F_q and F_t ; MR : Mated ridge pairs between F_q and F_t , and corresponding sampling points on them

- 1: $MR \leftarrow MRSP$
 - 2: Initialize the queue of candidate aligned ridge pairs, Q , based on $MRSP$
 - 3: **while** Q is not empty **do**
 - 4: Retrieve the first candidate aligned ridge pair in Q : CR
 - 5: $mrsp \leftarrow IntraRidgeMatch(CR)$
 - 6: **if** $|mrsp| > 4$ **then**
 - 7: Append $mrsp$ to MR
 - 8: Generate new candidate aligned ridge pairs based on $mrsp$
 - 9: Push the new candidate aligned ridge pairs into Q
 - 10: **end if**
 - 11: **end while**
 - 12: Calculate the similarity between the ridges in F_q and F_t : s_r
-

After the initialization of Q , we start the main loop of the Inter-Ridge propagation procedure to compare the ridges in each of the candidate aligned ridge pairs in Q until Q is empty. The first candidate in Q is popped out and matched by the Intra-Ridge matching procedure. If more than four mated sampling points are established, new candidate aligned ridge pairs are generated and pushed into Q . When Q is empty, the Inter-Ridge propagation procedure terminates with a set of mated ridge pairs as well as the

corresponding mated sampling points. Figs. 9(c) and 9(d) shows the mated ridge pairs found between the two example fingerprints as the procedure Inter-Ridge propagation proceeds from the mated ridge pairs shown in Fig. 9(b).

Let \bar{s}_N , \bar{d}_{loc} , and \bar{d}_{ori} be the average similarity between neighboring ridge structures of all the mated ridge pairs, the average location displacement and the average orientation difference between all the mated sampling points, respectively. Let n_{MRSP} and n_{RSP} denote the total number of mated sampling points on the ridges in the two fingerprints and the total number of sampling points on ridges in the query fingerprint, respectively. Then the similarity between the ridges in the two fingerprints is defined as

$$s_r = 0.3 \times \bar{s}_N + 0.2 \times \frac{10 - \bar{d}_{loc}}{10} + 0.2 \times \frac{15 - \bar{d}_{ori}}{15} + 0.3 \times \frac{n_{MRSP}}{n_{RSP}}. \quad (4)$$

3.3 Pore Matching

Once the correspondences between ridges are obtained, the level 3 features can be matched along the mated ridges. To implement this, we need to first associate the level 3 features with the ridges. In this section, we discuss the matching of pores; the matching of DIP features will be discussed in the next section. Recall that pores in a fingerprint are all located on ridges. Hence, for each pore, we find the closest ridge to it and its projection point on this ridge. The pores on the same ridge are then grouped together and ordered along the ridge tracing direction.

Given a pair of mated ridges, the correspondences between pores on these two ridges are found using the following method. For each pore on a ridge, POR_1 , we first find its closest sampling point SP_1 on the ridge (denote the ridge as R_1). If SP_1 does not have a mated sampling point, then POR_1 does not have any mated pores; otherwise, we find the nearest pore, POR_2 , to the mated sampling point, SP_2 , of SP_1 . The location displacement d_i between POR_i and SP_i ($i = 1, 2$) is calculated as the difference between the sampling indices of the projection point of POR_i and SP_i . The location displacement between the two pores, POR_1 and POR_2 , is then defined as $d_{loc} = |d_1 - d_2|$. If d_{loc} is smaller than a given threshold (i.e. 10 pixels for 1000ppi fingerprint images), POR_1 is mated with POR_2 . After all the pores in the latent are examined, we get the mated pores between the two fingerprints. Fig. 10(a) shows the mated pores obtained between a latent and its mated exemplar.

To calculate the pore match score, we compare the neighboring ridge structures and pore distribution of the mated pores on each pair of mated ridges (recall that the pores on a ridge are ordered, so are the mated pores). A comparison of neighboring ridge structures is the same as being described for mated sampling points on ridges (see Section 3.2.1). As for the neighboring pore distribution, if two

mated pores both have a neighboring pore on its left-hand side or right-hand side neighboring ridge, the location displacement between the neighboring pores is calculated. Let $d_{NP}^{l,i}$ be the location displacement between the neighboring pores on the left-hand side of the i_{th} mated pores on the mated ridges, and $d_{NP}^{r,i}$ the location displacement between the neighboring pores on the right-hand side of them. The similarity between the neighboring ridge structures and pore distribution of the mated pores in the two ridges can be then calculated as

$$s_N = 0.4 \times \frac{n_{NR}^l}{n_{mp} - 1} + 0.4 \times \frac{n_{NR}^r}{n_{mp} - 1} + 0.1 \times \frac{\sum_{i=1}^{n_{NP}^l} (10 - d_{NP}^{l,i})}{10 \times n_{NP}^l} + 0.1 \times \frac{\sum_{i=1}^{n_{NP}^r} (10 - d_{NP}^{r,i})}{10 \times n_{NP}^r}, \quad (5)$$

where n_{mp} is the number of mated pores on the two ridges and n_{NP}^l and n_{NP}^r are the number of cooccurring neighboring pores on the left-hand and right-hand sides, respectively. Finally, the pore match score between the two fingerprints is defined as

$$s_{POR} = 0.8 \times s_r + 0.2 \times (0.3 \times \bar{s}_N + 0.3 \times \frac{10 - \bar{d}_{loc}}{10} + 0.4 \times \frac{n_{MP}}{n_P}), \quad (6)$$

where \bar{s}_N is the average similarity between neighboring ridge structures and pore distribution of all the mated pores on the mated ridge pairs, \bar{d}_{loc} is the average location displacement between all the mated pores, and n_{MP} and n_P denote the total number of mated pores and the number of pores in the query latent fingerprint, respectively. It is worth mentioning that the above match score measures the similarity between fingerprints by considering not only the location displacement between mated pores and the number of mated pores, but also the consistency of the ridge structures and feature distribution surrounding the mated pores, whereas existing methods [10][12] consider only the location displacement or the number of mated pores.

3.4 DIP Matching

The matching of DIP features is also constrained along mated ridges. Unlike pores, DIP features reside on valleys rather than ridges. Therefore, we associate each DIP feature with two ridges that are on the left-hand and right-hand sides of the valley on which it resides. Given a DIP feature DIP_1 which is associated with two ridges R_{11} and R_{12} , the nearest sampling point to its projection on the ridge R_{11} is first found, denoted as SP_1 . If SP_1 does not have mated sampling points, then DIP_1 does not have mated DIP features; otherwise, the nearest DIP feature to the mated sampling point SP_2 on the mated ridge R_{21} of R_{11} is found, denoted as DIP_2 . Let d_i be the location displacement between DIP_i and SP_i ($i = 1, 2$), then the location displacement between DIP_1 and DIP_2 is $d_{loc} = |d_1 - d_2|$. Let R_{22} be the other ridge associated with DIP_2 . DIP_1 and DIP_2 are mated DIP features only if i) $d_{loc} \leq 10$ and

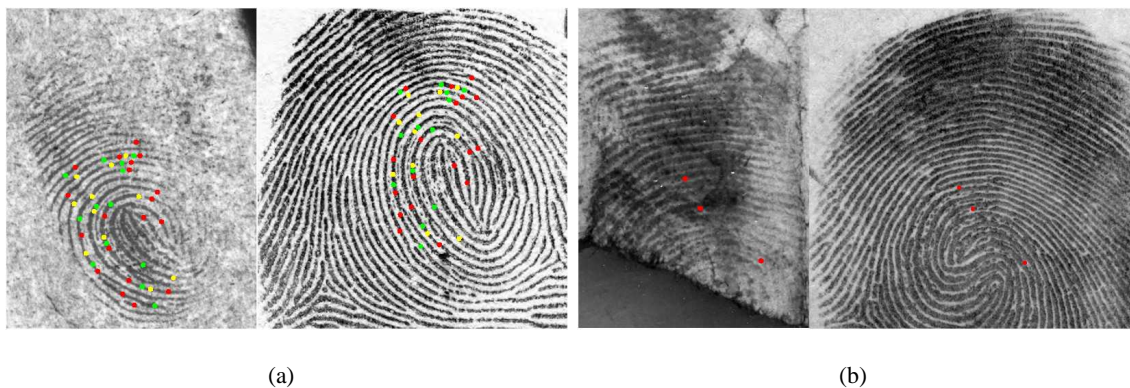


Fig. 10. Example level 3 feature matching results. (a) Mated pores in the latent shown in Fig. 3(b) and its mated exemplar. Corresponding pores are marked by the same color. (b) Mated DIP features in the latent shown in Fig. 9(a) and its mated exemplar.

ii) R_{12} and R_{22} are mated ridges. After enumerating all the DIP features in F_q , we obtain the mated DIP features. Fig. 10(b) shows the obtained mated DIP features in a latent and its mated exemplar.

Let \bar{d}_{loc} be the average location displacement between all the mated DIP features and n_{MDIP} and n_{DIP} be the total number of mated DIP features and the number of DIP features in the query latent fingerprint, respectively. The DIP match score between the two fingerprints is then defined as

$$s_{DIP} = 0.8 \times s_r + 0.2 \times \left(0.3 \times \frac{10 - \bar{d}_{loc}}{10} + 0.7 \times \frac{n_{MDIP}}{n_{DIP}} \right). \quad (7)$$

4 EXPERIMENTS

4.1 Databases

Two latent databases were used in this study. One is the ELFT-EFS-PC database [16], which has 242 1000 ppi latent fingerprints (most of them are from the same source as the latents in NIST SD27) with 1000 ppi mated full prints. The level 3 features in these latents have already been manually marked by latent examiners. The background database consists of 4,180 1000 ppi fingerprint images, which were collected from the mated fingerprints of the latents and the “B” session fingerprint images in the NIST SD29 and the NIST SD30 datasets. The second latent database was collected at West Virginia University (WVU). It has 127 latents in which the level 3 features have been manually marked. While these latents are at 1000 ppi, the full fingerprints in the background database are only at 500 ppi. In an earlier study [18], we investigated the utility of pores in the context of varying fingerprint image quality and resolution by using the rolled ink fingerprint images in NIST SD30 and a commercial minutiae matcher (VeriFinger

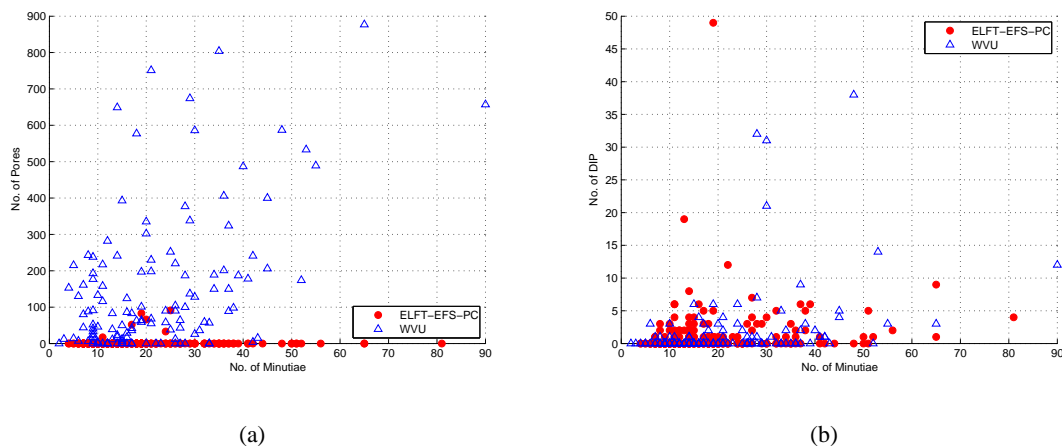


Fig. 11. The number of features in the latents in the ELFT-EFS-PC and WVU databases. (a) Number of pores vs. Number of minutiae. (b) Number of DIP features vs. Number of minutiae.

[19]). It was reported that automatic pore extraction and the resulting matching accuracy are significantly affected by fingerprint image quality. Further, it is only at high resolution (1000 ppi) and for good quality fingerprint images that the pores can improve the fingerprint verification accuracy, and even then only marginally. Hence, the WVU database is not suitable for studying the utility of level 3 features in latent matching (although many latents in it have large number of pores, the mated rolled images at 500 ppi do not have a sufficient number of pores), and we simply used it for reporting the statistics of level 3 features in latents.

4.2 Statistics of Level 3 Features in Latents

The statistics of level 3 features in the latents in the ELFT-EFS-PC and WVU databases have been collected based on the manual markup data. Fig. 11 shows the number of level 3 features (i.e. pores and DIP features) with respect to the number of minutiae. It can be seen that there is a large variance in the number of level 3 features across different latent fingerprints. In ELFT-EFS-PC, very few of the latents (only 6 of 242 latents) have any pores. Fig. 12 shows three example latents in ELFT-EFS-PC, which have 91, 17, and 0 pores marked by the latent examiners, respectively. Given such a small number of latents in ELFT-EFS-PC which have pores, pore matching is not likely to improve the latent matching accuracy on this database. Since no public domain latent database is suitable for studying the utility of pores, we constructed a simulated partial fingerprint database and investigated the effectiveness of pores on that dataset (see Section 4.5). On the other hand, many (79 out of 242) latents in ELFT-EFS-PC do

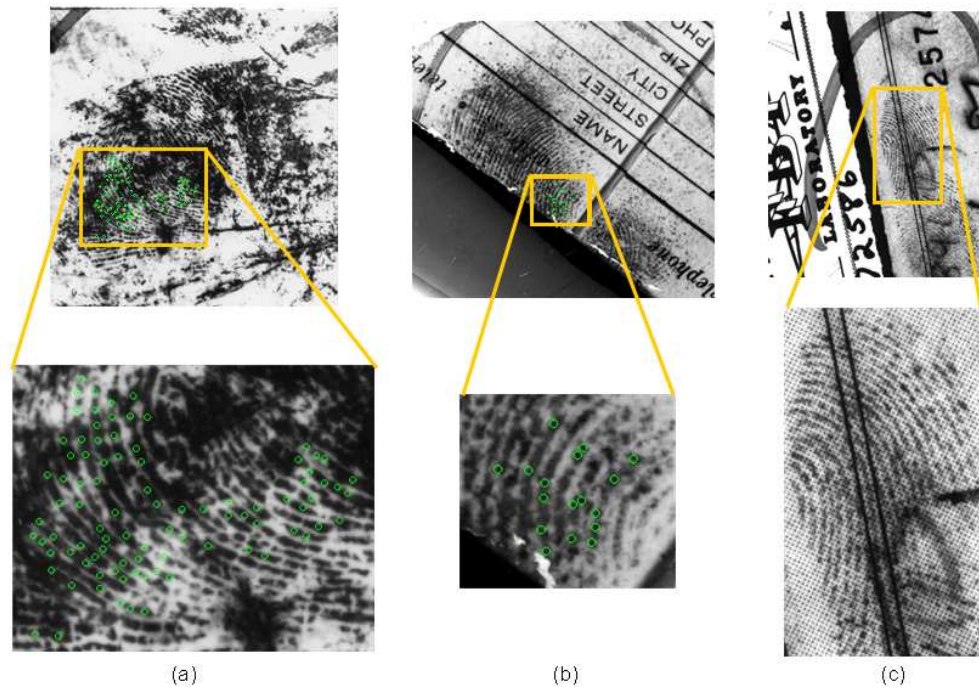


Fig. 12. Example latents in ELFT-EFS-PC with markup pores. (a) 91 pores, (b) 17 pores, and (c) 0 pores.

have DIP features. Therefore, we will use the ELFT-EFS-PC database for studying the effectiveness of DIP features.

4.3 Feature Detection Accuracy

Sixty partial fingerprints (320×240 pixels) were cropped from the 1000 ppi rolled ink fingerprint images ($\sim 1500 \times 1500$ pixels) in NIST SD30. The pores, dots, incipient ridges, and ridge edge protrusions in these sixty partial fingerprint images were manually marked for the purpose of evaluating their automatic detection accuracy. In order to study the impact of image quality on the automatic detection accuracy, the 60 partial fingerprint images were divided into two quality groups (good and bad) according to their image quality evaluated by the method in [22]. Two pore detection methods were considered, i.e. the proposed method and the method in [10]. These two methods differ in that the proposed method conducts filtering in the spatial domain using an anisotropic model, whereas the method in [10] applies filtering in the frequency domain with an isotropic model. Table 1 gives the average pore detection accuracy along with the standard deviation of the two methods on the ground truth dataset; R_t , the true detection

TABLE 1

Average pore detection accuracy and standard deviation

Method	Proposed		Method in [10]	
	Good	Bad	Good	Bad
$R_t(\%)$	73 ± 9.5	67 ± 14.6	69 ± 16.0	63 ± 12.5
$R_f(\%)$	20 ± 12.2	30 ± 14.4	27 ± 11.7	40 ± 18.1

TABLE 2

Average DIP detection accuracy and standard deviation

Quality	Good	Bad
N_m	6 ± 5.6	12 ± 8.5
N_s	4 ± 3.6	10 ± 7.0

rate, is defined as the ratio of the number of true detected pores to the total number of ground truth pores, and R_f , the false detection rate, is defined as the ratio of the number of falsely detected pores to the total number of detected pores. These results show that the detection accuracy of both the methods degrades as the fingerprint image quality goes down. As the fingerprint image quality changes from good to bad, the true detection rate decreases by about 5%, and the false detection rate increases more by about 10%. According to the standard deviation of the detection accuracy, in general, the automatic pore detection methods are more robust on good quality fingerprint images than on bad quality fingerprint images. Table 2 presents the detection accuracy of the proposed DIP detection method ([10] did not present a DIP feature extractor), where N_m and N_s denote the numbers of missing features and spurious features, respectively. Note that the average numbers of observable DIP features on good and bad quality fingerprint images in the ground truth dataset are 12 and 27, respectively. Again, poor quality fingerprint images cause more missing features as well as more spurious features. These results show that improving the quality of full fingerprint images in the background database is very important for the effectiveness of level 3 features in latent fingerprint matching. We will further demonstrate this in the next section.

4.4 Latent Fingerprint Matching

We have evaluated the latent matching performance with pores and DIP features on the 242 latents in ELFT-EFS-PC. Features (including minutiae, ridge skeletons, pores, and DIP) were manually marked in

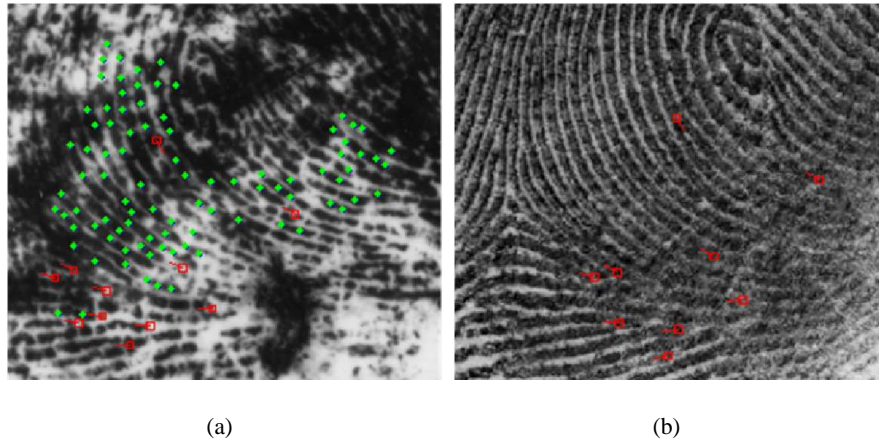


Fig. 13. Poor quality of exemplar fingerprints significantly degrades the utility of level 3 features. (a) Latent L030G in ELFT-EFS-PC, and (b) its mated full fingerprint image. Nine mated minutiae are found between them. But none of the 91 pores marked in the latent (as shown in (a)) have any corresponding pores in the mated full fingerprint.

latents, and automatically extracted from full fingerprints in the background database by using VeriFinger and the proposed level 3 feature extraction methods. As discussed in Section 3.1, level 3 features are matched only when the rank 1 minutiae match score of a latent is smaller than the given threshold (in our experiments, it was empirically set to 80 according to the raw match scores of VeriFinger on ELFT-EFS-PC, which ranged from 0 to 248). For the sake of efficiency, we matched level 3 features only between the latent and the top 100 candidate exemplars retrieved by VeriFinger. The match scores of VeriFinger and level 3 features were then combined by using the weighted sum rule [23]. Before the fusion, the minutiae match scores of each query latent fingerprint were normalized by using the max-min normalization method [23] based on the maximum and minimum scores between it and the exemplars.

According to the experimental results, among the 6 latents in ELFT-EFS-PC that have patron pores, three are already correctly identified at rank 1 by VeriFinger, two (L030G with 91 pores and L201U with 17 pores, see Figs. 12(a) and 12(b)) are correctly matched with their true mates after rank 1 but before rank 100, and the remaining one (L014G with 83 pores, see Fig. 3(b)) is correctly matched at rank 2874. By applying the proposed level 3 feature based latent matching method, however, the identification results of the latents L030G and L201U are not improved. This is because i) the number of pores is small or the pores are sparsely distributed in the latent (e.g. L201U), or ii) the corresponding region of the latent in its mated full fingerprint image is of poor quality and has few pores (e.g. L030G). Fig. 13

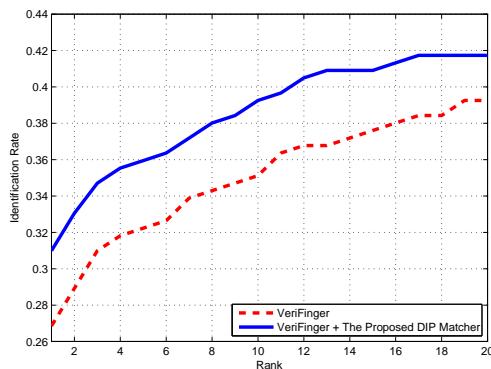


Fig. 14. Identification accuracies of VeriFinger and combination of VeriFinger and the proposed DIP matcher on the ELFT-EFS-PC database.

shows the latent L030G and its mated full fingerprint. Although there are nine mated minutiae in the two prints shown in Fig. 13, no corresponding pores are found in the full fingerprint for any of the markup pores in the latent. This is due to the poor quality of the corresponding region in the full fingerprint.

Fig. 14 presents the Cumulative Match Curves of VeriFinger and combination of VeriFinger and the proposed DIP matcher on the ELFT-EFS-PC database. At rank 1, VeriFinger correctly identified 65 latents; this number was improved to 75 after incorporating the proposed DIP matcher. In addition, many of the other latents had the ranks of their true mates improved. For example, for the latent shown in Fig. 10(b), its true mate was ranked at 82 by VeriFinger; after incorporating the proposed DIP matcher, the rank was improved to 4. From these results, we can see that level 3 features, when reliably present in both latents and their mated full fingerprints, are indeed useful in improving the latent matching accuracy.

Unfortunately, there are many difficulties in using level 3 features on the available latent databases. For one thing, there are very few latents in the latent databases with a sufficient number of level 3 features. This is not only because of the generally low quality of latent fingerprints, but also because latent experts often are not able to mark some of the level 3 features. While we can clearly see a large number of pores in the latent shown in Fig. 1(c), according to the markup data in ELFT-EFS-PC, three of the four latent experts did not mark any pores in it. Another concern is that the quality of the exemplar full fingerprints in these databases is not good enough to automatically extract reliable level 3 features. As a consequence, it is not possible to utilize the level 3 features even though they are present in latents (as shown in Fig. 13). Such a problem of reproducibility of level 3 features in exemplar full fingerprints has also been

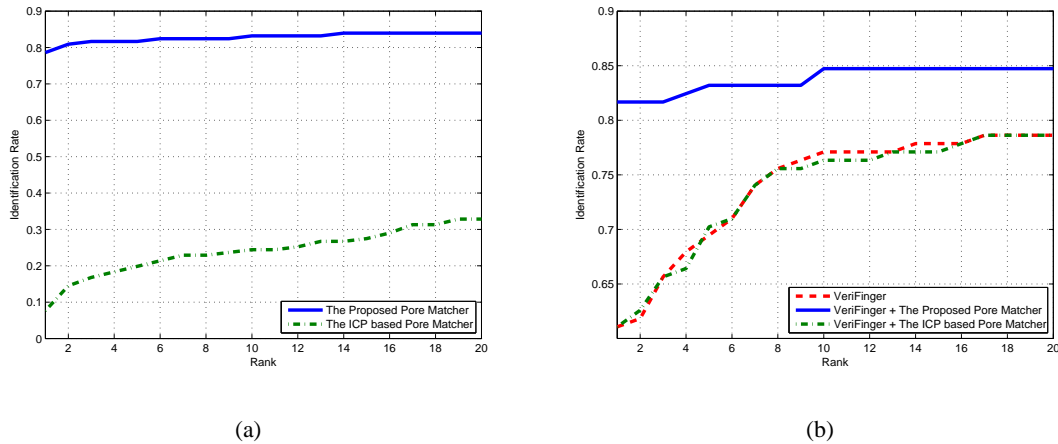


Fig. 15. Identification accuracy of the 131 simulated partial fingerprints and 4180 background exemplars. (a) Performance of the proposed pore matcher and the ICP based pore matcher. (b) Performance of combining VeriFinger and pore matchers.

acknowledged in a recent survey on level 3 features among latent examiners [25].

4.5 Simulated Partial Fingerprint Recognition

The experimental results presented above not only show the potential of level 3 features in improving latent matching accuracy, but also demonstrate the difficulty of using level 3 features in existing latent databases due to the small number of latents having level 3 features and the poor quality of mated full fingerprints. In order to better understand the utility of level 3 features, in particular pores, we constructed an additional set of 131 simulated partial fingerprint images of small area (320×240 pixels). They were cropped from the 1000ppi “B” session rolled ink fingerprint images ($\sim 1500 \times 1500$ pixels) in NIST SD30. The pores in these 131 partial fingerprints were manually marked, whereas the minutiae and ridge skeletons were extracted by VeriFinger [19]. The background database in the experiments was the same as in our experiments with ELFT-EFS-PC, except that the exemplars from the “B” session rolled ink fingerprint images in NIST SD30 were substituted with the corresponding “A” session images in the database (since the simulated partial fingerprint images as the query fingerprints were cropped from the “B” session images). All features in the exemplars were automatically extracted by VeriFinger and the proposed level 3 feature extraction methods. Next, we report the performance of the proposed pore matching method, and we compare it with VeriFinger and the ICP based pore matching method [10] to show the effectiveness of the proposed method and the utility of pores.

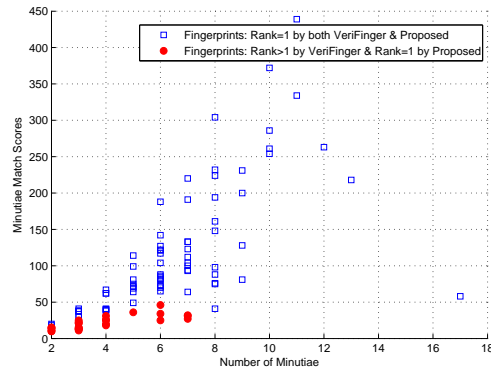


Fig. 16. Number of minutiae vs. the minutiae match scores in fingerprints with different identification results.

The identification accuracy on this dataset is presented in Fig. 15. Using VeriFinger, among the 131 query partial fingerprints, 80 fingerprints were correctly identified at rank 1. After incorporating the proposed pore matcher, 27 additional fingerprints were successfully identified at rank 1. Compared with the results on ELFT-EFS-PC, these results are much more promising; they show the effectiveness of level 3 features in matching partial fingerprints of small area which will otherwise pose a challenge to minutiae based AFIS due to the limited number of minutiae they contain. Moreover, the importance of collecting good quality full fingerprints can also be seen from these results. With the fast development of fingerprint imaging techniques and the widespread use of high resolution (1000 ppi) live-scan fingerprint scanners, we believe that it is becoming feasible to collect good quality fingerprints. This will facilitate extraction of reliable level 3 features and thereby further improve the latent matching accuracy of existing AFIS by incorporating level 3 features.

Fig. 16 compares the fingerprints which are correctly identified at rank 1 by both VeriFinger and the proposed method with those which are correctly identified after rank 1 by VeriFinger, but at rank 1 after incorporating the proposed method. Interestingly, the improvement due to level 3 features is only in situations where fingerprints have a small number of minutiae or low minutiae match scores. This indicates that i) minutiae matchers usually work very well when there is a sufficient number of minutiae, and ii) the contribution of level 3 features is more effective for fingerprints which have few minutiae or low minutiae match scores. In [25], about one-third of the participant latent examiners reported that they do not consider level 3 features when level 2 features are of sufficient quality and are sufficient in number, which confirms our findings here. Moreover, these observations also justify the proposed level

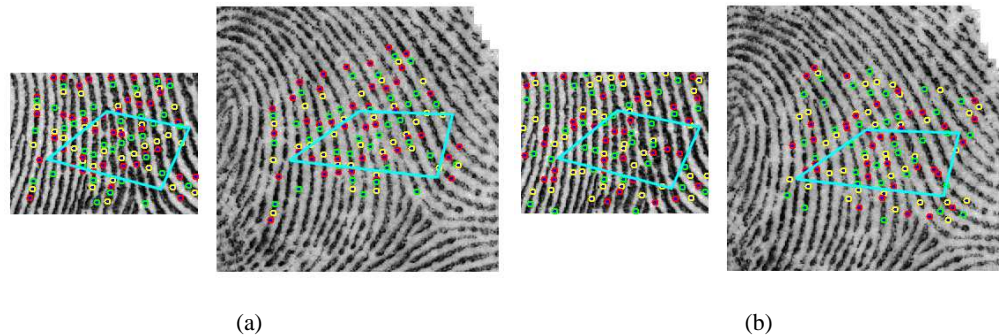


Fig. 17. Pore matching results on an example partial fingerprint and its mated full fingerprint (cropped for display purposes) by using (a) the proposed method and (b) the ICP based method. The polygons highlight the corresponding reference minutiae between the fingerprints. Due to the large distortion in the fingerprints, the ICP based method mis-matches many pores; on the contrary, the proposed method is more robust to distortion, and can still correctly match most of the pores.

3 feature based latent fingerprint matching algorithm sketched in Section 3.1.

For comparison, the ICP based level 3 feature matching method in [10] has also been implemented. Given a pair of mated minutiae between two fingerprints, the method in [10] first uses the two mated minutiae to align the level 3 features (here, pores) in the two fingerprints, and then employs the ICP algorithm to further align and match the level 3 features. The match score for the two fingerprints was finally computed based on the average distance, \bar{d} , between the obtained mated pores: $s_{POR} = 1 - \bar{d}/d_{Max}$, where d_{Max} is the maximum distance between mated pores (in our experiments, the distance threshold between two mated pores was set to 10 pixels). The CMC of the ICP based method in Fig. 15(a) shows that its performance is much worse than the proposed method: Only 10 fingerprints are correctly identified at rank 1. By fusing its scores with the scores of VeriFinger, we did not get consistent improvement in the identification accuracy (see Fig. 15(b)).

Fig. 17 shows the pore matching results on an example partial fingerprint and its mated full fingerprint (cropped for display purposes) by using the proposed method and the ICP based method, respectively. Obvious distortion can be observed between the two fingerprints (note the polygons highlight the corresponding minutiae). As a consequence, in the ICP based method, most pores are falsely matched (see Fig. 17(b)). On the contrary, most pores are correctly matched by the proposed method despite the large distortion (see Fig. 17(a)). Based on the match scores, the rank of the mated fingerprint in this pair is 1

(the proposed method) and 16 (the ICP based method), respectively, while VeriFinger ranks it at 5. These results illustrate the advantage of the proposed method in considering ridge structures and inter-feature topology when matching level 3 features in fingerprints.

5 CONCLUSIONS

We have studied the utility of level 3 features for latent fingerprint matching. Automatic algorithms have been proposed for extracting and matching several level 3 features, i.e. pores, dots, incipient ridges, and ridge edge protrusions. The proposed matching algorithm compares level 3 features along ridges, and enforces the topological relationship between level 3 features, minutiae, and ridges. It is thus more effective for latent fingerprints of small area and robust to distortion (on the set of simulated partial fingerprints, after combination with VeriFinger minutiae matcher, the rank 1 identification rate by the proposed method is $\sim 81.8\%$, whereas that by the existing ICP based method is $\sim 61.1\%$). Based on the performance of the proposed algorithms on operational latent databases and simulated partial fingerprints, we have shown that

- Published level 3 feature matching algorithms provide poor performance on operational latent fingerprint databases. Further, conclusions made by previous level 3 studies do not hold for challenging latent fingerprint matching problems;
- The limited number of latents that have level 3 features and the low reproducibility of level 3 features in poor quality exemplar full fingerprints make the level 3 features of limited use in improving the latent matching accuracy on the available latent databases;
- The latent matching accuracy can be improved by level 3 features if the features can be reliably extracted in both latents and mated full fingerprints (the rank 1 accuracy on the ELFT-EFS-PC database is improved from $\sim 26.9\%$ to $\sim 31\%$ after incorporating the proposed DIP matcher);
- The contribution of level 3 features is more effective when the number of minutiae in latents is small or the minutiae-based match score is low.

While the results of our study demonstrate the potential of level 3 features in improving latent matching accuracy, they also show the difficulties in using level 3 features. In order to better explore level 3 features in latent matching and to improve the latent matching accuracy of contemporary AFIS, we would like to make the following recommendations:

- Additional attention should be paid during enrollment to ensure that a sufficient number of level 3 features in fingerprints be captured. As observed in this study, poor quality of full fingerprints is one of the major reasons for limited contribution of level 3 features. Using high resolution (≥ 1000

ppi) scanners is a necessary but not a sufficient condition for extracting level 3 features. Fingerprint image quality assessment software that can provide real-time quality level estimates will be very useful. Since existing fingerprint image quality assessment algorithms (e.g. [22][26]) do not consider level 3 features, new fingerprint quality assessment algorithms need to be developed;

- Tiny latent fingerprints that have few minutiae but very clear level 3 features should not be simply discarded. As current AFIS generally cannot correctly identify latents with very few minutiae (say fewer than 6), more attention should be paid to them in terms of level 3 features, provided that a large percentage of level 3 features are available in them;
- Latent experts and AFIS developers should cooperate to form a consensus on how to mark level 3 features and ridge quality map in order to optimize the utility of level 3 features. As we observed in the ELFT-EFS-PC database, level 3 feature marking in many latents is not satisfactory from the viewpoint of AFIS developers. In addition, large inconsistency exists among different latent experts. The close cooperation between latent experts and AFIS developers will in the end help improve the fingerprint standard, such as CDEFFS [5];
- Use level 3 features only when it is necessary. Marking level 3 features in latents is time-consuming and tedious. Furthermore, when a large number of minutiae are available, the additive value of level 3 features is limited. A simple indicator for using level 3 features is when the minutiae match score at rank 1 is lower than a predefined threshold;
- ELFT-EFS evaluation would be more useful if the fingerprint image database was made open, and the utility of level 3 features was separately tested instead of being mixed with other extended features.

ACKNOWLEDGMENT

This work was supported by NIJ grant 2007-RG-CX-K183. The authors would also like to acknowledge the support provided by FBI Biometric Center of Excellence during this work.

REFERENCES

- [1] H. C. Lee and R. E. Gaensslen (eds.), *Advances in Fingerprint Technology*, 2nd ed. Elsevier, 2001.
- [2] D. Maltoni, D. Maio, A. K. Jain, and S. Prabhakar, *Handbook of Fingerprint Recognition*, 2nd ed. Springer-Verlag, 2009.
- [3] D. R. Ashbaugh, *Quantitative-Qualitative Friction Ridge Analysis: An Introduction to Basic and Advanced Ridgeology*. CRC Press, 1999.
- [4] A. Roddy and J. Stosz, "Fingerprint features - Statistical analysis and system performance estimates," *Proceedings of the IEEE*, vol. 85(9), pp. 1390-1421, 1997.

- [5] CDEFFS, *Data Format for the Interchange of Extended Fingerprint and Palmprint Features*, Draft Version 0.5, April 2010, <http://fingerprint.nist.gov/standard/cdeffs/index.html>.
- [6] SWGFAST, http://fingerprint.nist.gov/standard/cdeffs/Docs/SWGFAST_Memo.pdf, 2005.
- [7] FBI, *Electronic Fingerprint Transmission Specification (EFTS)*, Version 7.1, May 2005, <http://www.fbi.gov/hq/cjisd/iafis/efst71/cover.htm>.
- [8] J. D. Stosz and L. A. Alyea, "Automated system for fingerprint authentication using pores and ridge structure," *Proc. of SPIE*, San Diego, vol. 2277, pp. 210-223, 1994.
- [9] K. Kryszczuk, P. Morier, and A. Drygajlo, "Study of the distinctiveness of level 2 and level 3 features in fragmentary fingerprint comparison," *Proc. of Biometric Authentication Workshop, ECCV 2004*, pp. 124-133, 2004.
- [10] A. K. Jain, Y. Chen, and M. Demirkus, "Pores and ridges: Fingerprint matching using level 3 features," *IEEE Trans. PAMI*, vol. 29(1), pp. 15-27, 2007.
- [11] Q. Zhao, D. Zhang, L. Zhang, and N. Luo, "Adaptive fingerprint pore modeling and extraction," *Pattern Recognition*, vol. 43(8), pp. 2833-2844, 2010.
- [12] Q. Zhao, L. Zhang, D. Zhang, and N. Luo, "Direct pore matching for fingerprint recognition," *Proc. of ICB*, Italy, pp. 597-606, 2009.
- [13] Y. Chen and A. K. Jain, "Dots and incipients: Extended features for partial fingerprint matching," *Presented at Biometric Symposium*, BCC, Baltimore, September, 2007.
- [14] International Biometric Group, *Analysis of Level 3 Features at High Resolutions, Phase II - Final Report*, 2008, http://www.biometricgroup.com/reports/public/NIJ_QRFRP_2007-DN-BX-K239_Final_Report.pdf.
- [15] J. Zhou, F. Chen, N. Wu, and C. Wu, "Crease detection from fingerprint images and its applications in elderly people," *Pattern Recognition*, vol. 42(5), pp. 896-906, 2009.
- [16] M. Indovina and A. Hicklin, *ELFT-EFS NIST Evaluation of Latent Fingerprint Technologies: Extended Feature Sets, Evaluation #1, Preliminary Report*, Jan. 2010, <http://fingerprint.nist.gov/latent/ELFT-EFS/>.
- [17] A. K. Jain and J. Feng, "Latent fingerprint matching," *IEEE Trans. PAMI*, to appear, 2010, http://www.cse.msu.edu/rgroups/biometrics/Publications/Fingerprint/JainFeng_LatentFp_PAMI10.pdf.
- [18] Q. Zhao and A. K. Jain, "On the utility of extended fingerprint features: A study on pores," *Proc. of IEEE Workshop on Biometrics, CVPR*, June 2010.
- [19] Neurotechnology, VeriFinger SDK, <http://www.neurotechnology.com/verifinger.html>.
- [20] T. Lindeberg, "Feature detection with automatic scale selection," *International Journal of Computer Vision*, vol. 30(2), pp. 79-116, 1998.
- [21] J. Feng, Z. Ouyang, and A. Cai, "Fingerprint matching using ridges," *Pattern Recognition*, vol. 39(11), pp. 2131-2140, 2006.
- [22] H. Fronthaler, K. Kollreider, J. Bigun, J. Fierrez, F. Alonso-Fernandez, J. Ortega-Garcia, and J. Gonzalez-Rodriguez, "Fingerprint image-quality estimation and its application to multialgorithm verification," *IEEE Trans. IFS*, vol. 3(2), pp. 331-338, 2008.
- [23] A. Ross, K. Nandakumar, and A. K. Jain, *Handbook of Multibiometrics*. Springer, 2006.
- [24] National Institute of Standards and Technology, *NIST Biometric Image Software*, <http://www.nist.gov/itl/iad/ig/nbis.cfm>.
- [25] A. Anthonioz, N. Egli, C. Champod, C. Neumann, R. Puch-Solis, and A. Bromage-Griffiths, "Level 3 detail and their role in fingerprint identification: A survey among practitioners," *Journal of Forensic Identification*, vol. 58(5), pp. 562-589, 2008.
- [26] E. Tabassi, *Fingerprint Image Quality, NFIQ*, NISTIR 7151 ed., National Institute of Standards and Technology, 2004.